Optimisation of indoor hybrid PLC/VLC/RF communication systems

Yeduri Sreenivasa Reddy[1] ✉, Meenakshi Panda[1], Ankit Dubey[2], Abhinav Kumar[3], Trilochan Panigrahi[1], Khaled M. Rabie[4]

[1]Department of Electronics and Communication Engineering, NIT Goa, Ponda 403401, India
[2]Department of Electrical Engineering, IIT Jammu, Jammu 181221, India
[3]Department of Electrical Engineering, IIT Hyderabad, Hyderabad 502285, India
[4]School of Engineering, Manchester Metropolitan University, Manchester M15 6BH, UK
✉ E-mail: ysreenivasareddy@nitgoa.ac.in

Abstract: In this study, the authors propose a hybrid power line communication (PLC)/visible light communication (VLC)/radio frequency (RF) fronthaul with a fibre-based wired backhaul system to support massive number of smart devices (SDs). Since a signal-to-noise ratio-based access point (AP) association and bandwidth (BW) allocation for each SD do not necessarily improve the system capacity, they propose novel and efficient AP association and BW allocation strategies to maximise the sum rate capacity (SRC) of the hybrid system under consideration. An optimisation problem is formulated for the SRC with the AP association and BW allocation as the optimisation parameters and a hierarchical decomposition method is used to convert the non-linear optimisation problem into a set of convex optimisation problems. Then, the proposed strategies are used to solve the optimisation problem in an iterative manner until the SRC converges to an optimal value. Further, an analytical approximation for the BW allocated to each SD for a given AP association is derived using the Lagrangian multiplier method. The performance of the proposed system is evaluated through extensive numerical results. Moreover, the effect of the increased number of SDs on the optimal SRC is analysed.

1 Introduction

Connectivity in the indoor environment has become one of the most important aspects of our modern society. Radio frequency (RF) based communication system is one of the most commonly used technology for indoor connectivity. Due to availability and cost issues with RF spectrum, recently, several other technologies have come under consideration to achieve reliable and high data rate indoor connectivity. Light emitting diodes (LEDs), for instance, are widely used because of their enhanced colour render capability, long life time, and huge energy savings [1]. These LEDs can be used for indoor wireless communications, known as visible light communication (VLC), for various smart applications as discussed in [2]. Power line communications (PLCs) is another such technology that has gained considerable research attention in recent years due to the existing ubiquitous infrastructure. These PLC terminals can communicate through power lines, whereas, mobile devices have to connect via either RF or VLC interfaces [3].

The Internet of Things has led to the deployment of millions of smart devices (SDs) due to their vast applications [4]. Moreover, providing high data rates for these large numbers of SDs, using the conventional RF-based communication systems have become a challenging task, owing to the limited spectrum. Further, it has been shown that PLC, VLC, or RF alone cannot be an effective solution to provide high data rates [1]. To address this problem, the hybrid systems have been proposed in the literature with the coexistence of different communication systems.

The integration of PLC and RF for wireless relaying systems has been proposed for many applications including indoor, outdoor, and smart grids [5–9]. In [5], for instance, wireless relaying systems are integrated with PLC for long distance transmissions. This integration technique shows better robustness than using conventional PLC or RF for both long and short range communication. In addition, a hybrid wireless-broadband PLC (BPLC) system has been presented in [6] that utilises the medium voltage power line cables for offering broadband services to remote areas. In [7], a hybrid PLC/RF system has been considered to improve the range of the RF signals in a multi-storey building. Here, PLC links work as a backbone to pass the RF signals between multiple rooms and floors. In [8], the authors have proposed a multi-channel receiver-based hybrid PLC/RF communication system which has been analysed in terms of selection combining and maximal ratio combining methods for fading compensation. The capacity analysis of an amplify-and-forward (AF) relay-based cascaded PLC/RF system has been carried out in [9], where PLC and wireless users communicate with each other through these relays.

Integration of PLC and VLC technologies for various applications have been discussed in [3, 10–13]. The first integration proposal has been discussed in [3] which utilises ON/OFF keying for data modulation. Then, orthogonal frequency division multiplexing (OFDM) technique has been developed for hybrid PLC/VLC system to mitigate the interference and inter-symbol interference (ISI) [10]. In [11], OFDM modulation-based integrated BPLC and VLC communication systems has been proposed to provide e-health services inside hospitals. The performance of the OFDM with binary phase shift keying for sub-carrier modulation has been investigated in [12] for the cascaded BPLC and VLC communication systems that reduce the effect of impulsive noise and ISI. In [13], a survey on the opportunity of integrating PLC and VLC channels has been presented. The capacity analysis of an AF and decode-and-forward based hybrid PLC/VLC systems have been carried out in [14, 15], respectively. Here, the source node first transmits the information to the relay through a PLC link and then the relay node amplifies [14] or decodes [15] and forwards it to the destination node through a VLC link. A hybrid VLC and RF system has been considered in [16] for indoor environments which improves the per user average and outage throughput. A cascaded PLC/VLC system has been considered in [17] that is compatible to provide multiple services with different quality of service requirements. In [18], an energy efficient wireless communication network has been developed
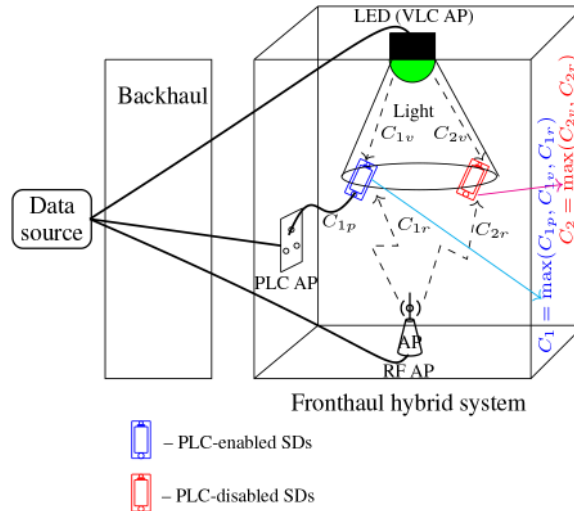
Fig. 1 *Hybrid PLC/VLC/RF system for indoor connectivity*

using both RF and VLC technologies to solve the power and BW allocation problem. An optimisation problem has been formulated in terms of power and bandwidth (BW) to maximise the energy efficiency of the heterogeneous network constrained by the maximum allowable transmit power from each access point (AP) and required data rates [18].

In [19], a cell breathing technique has been used for traffic transfer between the devices and APs in a cellular network. A pricing-based distributed algorithm has been used in [20] which considers congestion levels of the base stations (BSs) and the transmission environment of the mobile terminals as the parameters for load balancing in the heterogeneous network. The weighted sum-rate (WSR) maximisation for a wireless cellular network has been addressed in [21]. In [21], the prioritised and randomised algorithms have been proposed which are based on the coordinated scheduling and discrete power control and require limited information exchange and processing at each BS. The sum rate maximisation using a signal-to-interference-plus-noise ratio (SINR) approximation and the max–min weighted SINR optimisation for a wireless network has been proposed in [22]. A study on the linear filter design for maximising the WSR in the multiple input multiple output broadcast channel (MIMO-BC) has been carried out in [23]. The WSR problem in this study is solved as a weighted sum minimum mean square error-problem with optimised mean square error-weights. The robust beam forming approach has been used in [24] to calculate the WSR for a multi-cell massive MIMO downlink system. In [4], the authors have investigated achievable data rate of a hybrid system comprising of cascaded PLC/VLC system in coexistence with the RF system for a constrained transmit power. In this study, the authors have developed an algorithm that optimally divides the maximum allocated power among all three communication links such that the achievable data rate can be maximised [4]. Further, an investigation of power allocation problem has been carried out in [1] for hybrid PLC/VLC system in coexistence with RF in an indoor environment. In [1], the authors have analysed the transmit power minimisation problem with a constrained generalised quality of service requirement. Then, for a constrained data rate requirement, a comparative analysis has been presented to exploit the benefits of a hybrid system in comparison to the existing RF system [1].

The hybrid systems that have been proposed in [1, 4], and [18] assumed that the mobile nodes are connected to both cascaded PLC/VLC and RF links and the high data rates are achieved through simultaneous transmissions from both the links. However, a massive number of SDs that require moderate data rates need to have number of resources. Further, it has also been noticed that the combination of fronthaul VLC and backhaul PLC is inefficient due to the relatively low data rate support of PLC [4]. Moreover, the PLC link can also be used to connect SDs due to the limited interference from the wireless links. To resolve this issue, we

propose a hybrid PLC/VLC/RF fronthaul with a fibre-based wired backhaul system, as the fibre-based link can provide very high data rate as shown in Fig. 1. Here, we consider two types of SDs namely PLC-enabled and PLC-disabled. The PLC-enabled SDs have signal reception interfaces for PLC, VLC, and RF, whereas, the PLC-disabled SDs have reception interfaces for VLC and RF only. Moreover, the optimisation of the sum rate capacity (SRC) with AP association and BW allocation is an open problem [18] and to the best of our knowledge, it has not been carried out for the hybrid PLC/VLC/RF system. Thus, in this work, a joint distribution algorithm based on (i) worst device reshuffling and (ii) load balancing techniques are proposed, in order to maximise the achievable SRC for the fronthaul hybrid PLC/VLC/RF communication system with a fixed transmit power from all APs. The key contributions of this work are as follows:

- The AP association and BW allocation for the hybrid PLC/VLC/RF system has been formulated as an optimisation problem.
- The presence of impulsive noise in the PLC system adds non-linearity to the optimisation problem compared to conventional cellular systems. Thus, a hierarchical decomposition method is considered to convert the resultant non-linear optimisation problem into a set of convex optimisation problems.
- A joint distribution algorithm based on (i) worst device reshuffling and (ii) load balancing techniques are proposed, to maximise the achievable SRC.
- An analytical approximation for the BW allocated to each SD for a given AP association is derived.
- A numerical analysis is presented on the achievable SRC to study the effect of increased number of PLC-disabled SDs.
- Finally, the effect of increased number of SDs on the optimal SRC is analysed numerically.

The rest of the paper is outlined as follows. The channel models corresponding to PLC, VLC, and RF are presented in Section 2. The proposed joint association and BW allocation is discussed in Section 3 and the performance of the proposed joint distribution algorithm is evaluated through extensive simulations in Section 4. Finally, Section 5 provides concluding remarks along with possible future scope.

2 System model

We consider an indoor downlink scenario with 1 RF AP, k VLC APs, l PLC APs, and N SDs. Let $a \in \mathcal{A} = \{0, 1, \ldots, k, k+1, \ldots, k+l\}$ denote the set containing the indices of RF, VLC, and PLC APs, where $a = 0$ denotes the index of RF, $a \in \{1, 2, \ldots, k\}$ denote the indices of VLC AP, and $a \in \{k+1, k+2, \ldots, k+l\}$ denote the indices of PLC AP. For convenience, let $n \in \mathcal{U} = \{1, 2, \ldots, N\}$ denote the set of SDs. In

this work, we assume two kinds of SDs such as PLC-enabled and PLC-disabled as shown in Fig. 1. The PLC-enabled SDs have signal reception interfaces for PLC, VLC, and RF, whereas, the PLC-disabled SDs have reception interfaces for VLC and RF only [1, 4]. Further, we assume that an SD can connect to only one AP using only one communication link at a given time. The channel models corresponding to PLC, VLC, and RF are presented in the following subsection. Moreover, we consider the effect of both attenuation and fading in the channel for the SRC analysis.

2.1 PLC channel model

In the PLC system, in addition to the distance dependent signal attenuation, fading, and impulsive noise also affect the transmitted data. Thus, in this work, we consider the effect of both channel impairments. The fading gain of the PLC channel can be modelled by a log-normal distribution [25–27]. Let P_T (in dB), P_R (in dB), and α (in dB/distance) denote the transmitted power, received power, and the attenuation factor with distance, respectively. Then, P_R can be expressed as [28]

$$P_R = P_T - \alpha d, \tag{1}$$

where d is the distance in the power line between the PLC AP and SD.

The fading amplitude h_p of the PLC channel is modelled as an independent and identically distributed (i.i.d.) log-normal random variable with probability density function (PDF) given as [29]

$$f_{h_p}(\nu) = \frac{1}{\nu\sqrt{2\pi\sigma_{h_p}^2}}\exp\left(-\frac{(\ln\nu - \mu_{h_p})^2}{2\sigma_{h_p}^2}\right), \quad \nu \geq 0, \tag{2}$$

where μ_{h_p} and $\sigma_{h_p}^2$ are the mean and variance of the normal random variable $\ln(h_p)$, respectively. Thus, the mth moment of h_p can be obtained as [30]

$$E[h_p^m] = \exp\left(m\mu_{h_p} + \frac{m^2\sigma_{h_p}^2}{2}\right), \tag{3}$$

where $E[\,\cdot\,]$ represents the expectation operator. Then, the average channel gain of the PLC channel is given as [31]

$$G_p = E[h_p^2] = \exp\left(2\mu_{h_p} + 2\sigma_{h_p}^2\right). \tag{4}$$

Unlike the other communication systems, power lines are subject to impulsive noise along with background noise. The prior noise occurs due to the switching transients at irregular intervals whereas the later occurs from the household appliances such as televisions, computers etc. [32, 33]. This mixture of noise can be well modelled by a Bernoulli-Gaussian process and its samples can be obtained as

$$n_p = n_g + n_b n_i, \tag{5}$$

where n_g and n_i represent the zero mean additive white Gaussian noise (AWGN) random variables with variances σ_g^2 and σ_i^2, respectively, and n_b represents the Bernoulli random variable with parameter ξ. Furthermore, as all samples have different origins, they are assumed to be independent. Therefore, the noise power spectral density, N_p (watts/Hz), can be obtained as

$$N_p = E[n_p^2] = \sigma_g^2(1 + \xi\gamma), \tag{6}$$

where $\gamma = \sigma_i^2/\sigma_g^2$ represents the power ratio of impulsive noise to the background noise. With this in mind, the corresponding SNR is given as [34]

$$\Gamma_p = (1 - \xi)\Gamma_1 + \xi\Gamma_2, \tag{7}$$

where Γ_1 and Γ_2 are given as

$$\Gamma_1 = \frac{P_R G_p}{\sigma_g^2 B_p}, \tag{8}$$

$$\Gamma_2 = \frac{P_R G_p}{\sigma_g^2(1 + \gamma)B_p}, \tag{9}$$

respectively, where B_p is the allocated BW.

2.2 VLC channel model

In the VLC system, there exist point-to-point and diffusing links between the LED and photodetector. In the primary links, the AP directly communicates with the devices and requires no obstacles present between them. Thus, in point-to-point links, the beams are directly pointed in the right directions. This, in turn, reduces the interference, attenuation, and results in higher data rate transmissions. Further, these links are very sensitive to blocking and shadowing effects as they require line-of-sight (LoS) transmission. In the secondary links, the signal radiates in accordance with a wide angle that is similar to RF links. Thus, these links suffer a loss in data rate and introduce multipath induced signal distortion, which significantly degrades the overall channel capacity. The multipath fading, which is common in traditional RF channels, does not significantly impact the VLC channel. This is because the signal wavelength in VLC is only hundreds of nanometres, and the size of commonly used photodetectors is in the order of few centimetres, which is sufficiently large to achieve effective space diversity for VLC signals, thereby mitigating the multipath fading [35]. In this work, we assume that all the VLC links are point-to-point and the corresponding channel gain is obtained as [36, 37]

$$H(0) = \begin{cases} \frac{(\rho + 1)A_d}{2\pi d^2}\cos^\rho(\delta)T_s(\beta) \\ \times\, g(\beta)\cos(\beta), & 0 \leq \beta \leq \beta_c \\ 0, & \beta \geq \beta_c, \end{cases} \tag{10}$$

where A_d denotes the area of the photodetector (SD), d is the distance between the VLC AP and the SD, δ is the angle between the light emitting direction and the light source normal direction, β represents the incident angle of radiation, $T_s(\beta)$ and $g(\beta)$ are the gains of optical filter and concentrator, respectively, β_c is the field of view of the receiver, and ρ represents the order of Lambert index which is obtained as [38, 39]

$$\rho = \frac{\log(1/2)}{\log(\cos(\psi))}, \tag{11}$$

where ψ is the LED's semi-angle at half power. Let P_T be the transmitted power and P_R the received power. Then, the received power can be expressed as [35]

$$P_R = H(0)P_T. \tag{12}$$

Hence, the corresponding SNR is given as [40]

$$\Gamma_v = \frac{(RP_R)^2}{N_v B_v}, \tag{13}$$

where B_v is the allocated BW, R the photodiode responsivity, and N_v, the noise power spectral density in watts/Hz with variance σ_v^2. In VLC, the total noise is a combination of the shot noise (σ_s^2) and the thermal noise (σ_T^2). However, the shot noise that is generated from ambient light is dominant compared to the thermal noise [40] and is obtained as [35, 38]

$$\sigma_s^2 = 2qR(P_R + P_n)B_n + 2qiI_2B_n, \tag{14}$$

where B_n and P_n are the noise-BW and noise power due to inter-symbol-interference (ISI), respectively, q is the electronic charge, i is the background current, and I_2 is the noise BW factor. Further, we assume that $P_n = 0$ as the VLC system is less sensitive to ISI [38].

2.3 RF channel model

In the RF system, the attenuation is modelled using the log-distance path loss model and fading is modelled using Rayleigh distribution. LoS path loss follows a relation defined as [40]

$$\eta[\text{dB}] = E\log_{10}(d) + F + G\log_{10}\left(\frac{f_c}{5}\right), \tag{15}$$

where d is the distance between the AP and SD, f_c is the carrier frequency in GHz, and $E = 18.7$, $F = 46.8$ and $G = 20$ are constants dependant on the propagation model. Then, the path gain is given as

$$G_{\eta,r} = 10^{-\eta[\text{dB}]/10}. \tag{16}$$

The fading amplitude h_r of the RF channel is modelled as i.i.d. Rayleigh random variable with mean $\sqrt{(\pi/2)}\sigma_{h_r}$ and variance $((4-\pi)/2)\sigma_{h_r}^2$. Thus, the corresponding PDF is given by [41]

$$f_{h_r}(\nu) = \frac{\nu}{\sigma_{h_r}^2}\exp\left(-\frac{\nu^2}{2\sigma_{h_r}^2}\right), \quad \nu \geq 0, \tag{17}$$

and the corresponding average channel gain $G_{h,r} = E[h_r^2] = 2\sigma_{h_r}^2$. Further, the noise in this channel model is assumed to be AWGN with mean zero and variance $\sigma_{A_r}^2$ and the noise power spectral density $N_r = E[n_r^2] = \sigma_{n_r}^2$. Hence, the corresponding SNR is expressed as

$$\Gamma_r = \frac{P_T G_{\eta,r} G_{h,r}}{N_r B_r}, \tag{18}$$

where P_T and B_r are the transmit power and allocated BW, respectively. Next, we frame the joint association and BW allocation for the PLC/VLC/RF system as an optimisation problem.

3 Joint association and BW allocation

In this section, we present the SRC, C, as a function of association and BW allocation. Wherein, we formulate a constrained optimisation problem of C with AP association and BW allocation as the optimisation parameters. After that, hierarchical decomposition method is used to solve the optimisation problem. Finally, we present the proposed joint distribution algorithm that improves the overall SRC of the proposed system.

3.1 Problem formulation

Let $\Lambda_{a,n}$ be the binary indicator that denotes the association of the SD to the RF channel for $a = 0$, VLC channel for $a \in \{1, 2, \ldots, k\}$, and PLC channel for $a \in \{k+1, k+2, \ldots, k+l\}$. Thus, the relation is obtained as

$$\sum_{a=0}^{k+l} \Lambda_{a,n} = 1, \quad \forall n \in \mathscr{U}, \tag{19}$$

which represents the consideration that each SD should associate with only one AP that belongs to only one communication technology. Thus, the SRC can be obtained as [42]

$$C = \sum_{a=0}^{k}\sum_{n=1}^{N} \Lambda_{a,n} B_{a,n}\log_2\left(1 + \frac{\Gamma_{a,n}}{B_{a,n}}\right) + \sum_{a=k+1}^{k+l}\sum_{n=1}^{N} \Lambda_{a,n} B_{a,n}\left[(1-\xi)\log_2\left(1 + \frac{\Gamma_{1_{a,n}}}{B_{a,n}}\right)\right. \tag{20}$$
$$\left. + \xi\log_2\left(1 + \frac{\Gamma_{2_{a,n}}}{B_{a,n}}\right)\right],$$

where $B_{a,n}$ represents the BW allocated by RF AP ($a = 0$), or VLC AP ($a = \{1, 2, \cdots, k\}$), or PLC AP ($a = \{k+1, k+2, \cdots, k+l\}$), to the SD $n \in \mathscr{U}$. In (20), the first summation term corresponds to RF and VLC and the second summation term corresponds to PLC. Since both RF and VLC share the same capacity expression, we have used a single set to denote both. However, we denote the PLC with a different set as it shares a different capacity expression from the VLC and RF due to the presence of impulsive noise. Thus, the optimisation problem for achieving the maximum SRC can be formulated as

$$\mathbf{P}: \max_{\Lambda, B} \ C(\Lambda_{a,n}, B_{a,n}) \tag{21}$$

$$\text{subject to } \sum_{a=0}^{k+l} \Lambda_{a,n} = 1, \ \forall n \in \mathscr{U}, \tag{22}$$

$$\sum_{n=1}^{N}(\Lambda_{a,n}B_{a,n}) \leq B_{a,\max}, \text{ for each } a \in \mathscr{A}, \tag{23}$$

$$B_{a,n} \geq 0, \tag{24}$$

The constraint in (22) is required as we consider the case that an SD can only associate to either of PLC/VLC/RF links. The constraint in (23) upper bound the BW available with each AP, respectively. The constraint in (24) ensures that the allocated BW to an SD has to be non-negative. The optimisation problem in (21) is a non-linear programming problem with association and BW allocation as the optimisation parameters [43]. It should be noted that it is difficult to solve this problem. Thus, in the following subsection, we discuss the hierarchical decomposition method [44] to solve the above non-linear optimisation problem in (21).

3.2 Hierarchical decomposition method

We can relax $\Lambda_{a,n}$ in $\mathbf{P}$, which gives

$$0 \leq \Lambda_{a,n} \leq 1 \ \forall (a,n) \in (\mathscr{A}, \mathscr{U}), \tag{25}$$

where the fractional value of $\Lambda_{a,n}$ denotes the partial AP association with different APs during AP association period. Initial step of this method is an upper level primal decomposition that decomposes $\mathbf{P}$ into $\mathbf{P1}$ and $\mathbf{P2}$. Here, $\mathbf{P1}$ is the optimisation problem of SRC with the association as the optimisation variable for a given BW. Further, $\mathbf{P2}$ is the optimisation problem of SRC with BW as the optimisation variable for a given association. For a given $B_{a,n}$, the optimisation problem $\mathbf{P1}$ can be obtained as

$$\mathbf{P1}: \max_{\Lambda_{a,n}} \ C(\Lambda_{a,n}, B_{a,n}^*)\forall (a,n) \in (\mathscr{A}, \mathscr{U}) \tag{26}$$

$$\text{subject to } \sum_{a=0}^{k+l} \Lambda_{a,n} = 1, \ \forall n \in \mathscr{U}. \tag{27}$$

Similarly, for a given $\Lambda_{a,n}^*\forall (a,n) \in (\mathscr{A}, \mathscr{U})$, the optimisation problem $\mathbf{P2}$ can be derived as

$$\mathbf{P2}: \max_{B_{a,n}} \ C(\Lambda_{a,n}^*, B_{a,n})\forall (a,n) \in (\mathscr{A}, \mathscr{U}) \tag{28}$$

subject to $\sum_{n=1}^{N} B_{a,n} \leq B_{a,\max}$, for each $a \in \mathscr{A} \ \& \ n \in \mathscr{U}_a$, (29)

$$B_{a,n} \geq 0,$$ (30)

where $B_{a,\max}$ denotes the maximum available BW with each AP $a \in \mathscr{A}$. Furthermore, for a given association, each AP present in the scenario gets the information about the number of SDs that are associated to it and has to optimally divide the BW, $B_{a,\max}$, available with it. Hence, the problem **P2** can be further simplified into **P21**$_a$ for each $a \in \{0,1,\ldots,k\}$ and **P22**$_a$ for each $a \in \{k+1,k+2,\ldots,k+l\}$ which are defined, respectively, as

P21$_a$: $\max_{B_{a,n}} \ \sum_{n \in \mathscr{U}_a} B_{a,n} \log_2 \left(1 + \frac{\Gamma_{a,n}}{B_{a,n}}\right)$ (31)

subject to $\sum_{n \in \mathscr{U}_a} B_{a,n} = B_{a,\max}$, (32)

$$B_{a,n} \geq 0,$$ (33)

P22$_a$: $\max_{B_{a,n}} \ \sum_{n \in \mathscr{U}_a} B_{a,n} \left[(1-\xi)\log_2\left(1 + \frac{\Gamma_{1_{a,n}}}{B_{a,n}}\right)\right.$
$$\left. + \xi \log_2\left(1 + \frac{\Gamma_{2_{a,n}}}{B_{kn}}\right)\right]$$ (34)

subject to $\sum_{n \in \mathscr{U}_a} B_{a,n} = B_{a,\max}$, (35)

$$B_{a,n} \geq 0.$$ (36)

Here, **P21**$_a$ corresponds to RF or VLC and **P22**$_a$ corresponds to PLC as they share different SRC expression. The optimisation problems defined in **P21**$_a$ for each $a \in \{0,1,\ldots,k\}$ are concave optimisation problems the dual of which is a convex optimisation problem. Thus, the duality of the optimisation problem **P21**$_a$ can be obtained as

$$f(\boldsymbol{B}_a) = \min_{B_{a,n}} \ \sum_{n \in \mathscr{U}_a} -B_{a,n}\log_2\left(1 + \frac{\Gamma_{a,n}}{B_{a,n}}\right)$$ (37)

subject to $g(\boldsymbol{B}_a) = \sum_{n \in \mathscr{U}_a} B_{a,n} - B_{a,\max} = 0$, (38)

where $\boldsymbol{B}_a$ is a vector of BWs allocated to each SD $n \in \mathscr{U}_a$, i.e. to each SD that is associated to AP a. In this work, the Lagrange multiplier method is used to solve the minimisation of convex optimisation problem defined in (37) with equality constraint on the BW defined in (38) [45]. Algorithm 1 (see, Fig. 2) shows the steps involved in the Lagrange multiplier method. Let $L_1(\boldsymbol{B}_a, \Omega_1)$ denotes the Lagrangian of the convex optimisation problem which is obtained as

---

Require: The minimization function $f(B_a)$, equality constraint $g(B_a)$
Ensure: Optimal value of BW allocation
   Compute $L(B_a, \Omega) = f(B) + \Omega g(B)$ with Ω as the Lagrange multiplier
   Compute $\nabla_B L(B_a, \Omega)$ and $\nabla_\Omega L(B_a, \Omega)$
   Assume $\nabla = \begin{bmatrix} \nabla_B \\ \nabla_{\Omega_a} \end{bmatrix}$
   Solve $\nabla L(B_a, \Omega) = 0$ to obtain the optimal values of $B_{a,n}$ for each $n \in \mathscr{U}_a$ and Ω

Fig. 2 *Algorithm 1: Lagrange multiplier method to obtain the optimal BW allocation*

$$L_1(\boldsymbol{B}_a, \Omega_1) = \sum_{n \in \mathscr{U}_a} B_{a,n}\log_2\left(1 + \frac{\Gamma_{a,n}}{B_{a,n}}\right)$$
$$+ \Omega_1\left(\sum_{n \in \mathscr{U}_a} B_{a,n} - B_{a,\max}\right).$$ (39)

where Ω_1 denotes the Lagrangian multiplier. Then, obtaining the partial derivatives of $L_1(\boldsymbol{B}_a, \Omega_1)$ with respect to each variable in $\boldsymbol{B}_a$ as well as Ω_1 and equating the result to zero which are obtained as

$$\nabla_{B_{a,n}} L_1(\boldsymbol{B}_a)$$
$$= \log_2\left(1 + \frac{\Gamma_{a,n}}{B_{a,n}}\right) - \frac{\Gamma_{a,n}}{\Gamma_{a,n} + B_{a,n}} + \Omega_1 = 0,$$ (40)

$$\nabla_{\Omega_1} L_1(\boldsymbol{B}_a) = \sum_{n \in \mathscr{U}_a} B_{a,n} - B_{a,\max} = 0,$$ (41)

Finally, by solving the linear equations defined in (40) and (41), with an assumption that $\Gamma_{a,n}/B_{a,n} \gg 1$, the optimal values of $B_{a,n}$ and Ω_1 are obtained as

$$B_{a,n} \simeq \frac{\Gamma_{a,n}B_{a,\max}}{\sum_{i \in \mathscr{U}_a} \Gamma_{a,i}}, \quad n \in \mathscr{U}_a,$$ (42)

$$\Omega_1 \simeq \log_2\left(\frac{\exp(1)B_{k,\max}}{\sum_{i \in \mathscr{U}_a} \Gamma_{a,i}}\right),$$ (43)

respectively, as shown in Algorithm 1 (Fig. 2). Similarly, from **P22**$_a$ derived in (34), it is observed that the first and second terms in the summation are also concave functions. The dual of each of these terms is a convex function. Thus, according to the additive property of convex functions [45], **P22**$_a$ is also a convex minimisation problem. Therefore, similar to **P21**$_a$, **P22**$_a$ can also be solved using the Lagrange multiplier method and the corresponding Lagrangian is defined as

$$L_2(\boldsymbol{B}_a) = \sum_{n \in \mathscr{U}_a} B_{a,n}\left[(1-\xi)\log_2\left(1 + \frac{\Gamma_{1_{a,n}}}{B_{a,n}}\right)\right.$$
$$\left. + \xi \log_2\left(1 + \frac{\Gamma_{2_{a,n}}}{B_{a,n}}\right)\right]$$
$$+ \Omega_2\left(\sum_{n \in \mathscr{U}_a} B_{a,n} - \boldsymbol{B}_{a,\max}\right).$$ (44)

where Ω_2 is the Lagrangian multiplier. Then, the partial derivatives are obtained as

$$\nabla_{B_{a,n}} L_2(\boldsymbol{B}_a)$$
$$= (1-\xi)\log_2\left(1 + \frac{\Gamma_{1_{a,n}}}{B_{a,n}}\right) - \frac{(1-\xi)\Gamma_{1a,n}}{\Gamma_{1_{a,n}} + B_{a,n}}$$
$$+ \xi\log_2\left(1 + \frac{\Gamma_{2_{a,n}}}{B_{a,n}}\right) - \frac{\xi\Gamma_{2a,n}}{\Gamma_{2_{a,n}} + B_{a,n}} + \Omega_2 = 0,$$ (45)

$$\nabla_{\Omega_2} L_2(\boldsymbol{B}_a) = \sum_{n \in \mathscr{U}_a} B_{a,n} - B_{a,\max} = 0.$$ (46)

Finally, the analytical approximations to optimal values of $B_{a,n}$ and Ω_2 are obtained by solving the linear equations defined in (45) and (46) with an assumption that $\Gamma_{1_{a,n}}/B_{a,n} \gg 1$ and $\Gamma_{2_{a,n}}/B_{a,n} \gg 1$ and are given as

$$B_{a,n} \simeq \frac{\Gamma_{1_{a,n}}^{(1-\xi)}\Gamma_{2,n}^{\xi}B_{a,\max}}{\sum_{i \in \mathscr{U}_a} \Gamma_{1_{a,i}}^{(1-\xi)}\Gamma_{2_{a,i}}^{\xi}}, \quad n \in \mathscr{U}_a,$$ (47)

$$\Omega_2 \simeq \log_2\left(\frac{\exp(1)B_{a,\max}}{\sum\limits_{i \in \mathcal{U}_a} \Gamma_{1_{a,i}}^{(1-\xi)}\Gamma_{2_{a,i}}^{\xi}}\right), \tag{48}$$

respectively, as shown in Algorithm 1 (Fig. 2).

3.3 Joint distribution algorithm

Fig. 3 shows the flowchart of the joint distributed algorithm that solves **P** in an iterative manner. Let $\mathcal{D}$ represents the set of PLC-disabled SDs in the system and $\mathcal{D} = \{0\}$ represents the case where all SDs are PLC-enabled. An SNR-based initial association is considered for Λ where the SD associated to an AP from which it receives maximum SNR, this solves the problem **P1**. Thereafter, for a known Λ, the problem is simplified to solving **P2** which is equal to obtaining the optimal values of BW allocated to each SD for a given association. These optimal values are obtained by solving the Lagrange equations in (39) and (44) and the approximate solutions are derived in (42) and (47), respectively. Finally, the SRC can be obtained from (20) using the association and the corresponding BW. The maximum SRC is obtained by using iterative-based reshuffling method. This iterative approach is based on two variants: (**V1**) reshuffling of the SD with the lowest
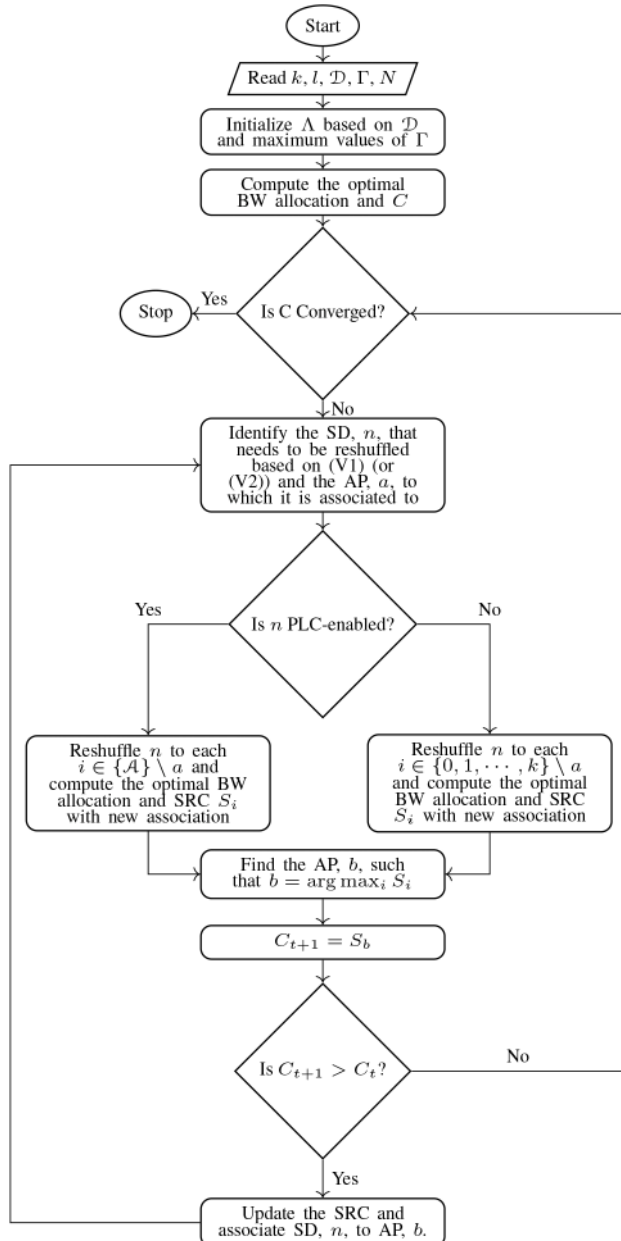

Fig. 3 *Optimal resource allocation*

SRC among all the SDs present in the hybrid system (worst device reshuffling technique) and (**V2**) reshuffling of the SD with the lowest SRC among all the SDs that belong to the AP with highest load (load balancing technique).

In the iterative-based reshuffling method, the initial step is to find the SD n that needs to be reshuffled based on (V1) (or (V2)) and the AP a to which it is associated. In case $n \in \mathcal{D}$, partially associate n to all the APs in the set $\{0, 1, \ldots, k\} \smallsetminus a$. Otherwise, partially associate u to all the APs in the set $\{\mathcal{A}\} \smallsetminus a$. In each case find the optimal values of BW and corresponding SRC. Let C_{t+1} be the maximum of all the sum rate capacities obtained in each partial association. In case $C_{t+1} > R_t$, then associate the SD to the AP that results in maximum SRC. Repeat the above procedure until the SRC convergences to a stable value.

4 Numerical results

Numerical results are presented in this section to compare the performance of the proposed hybrid communication system with hybrid PLC/VLC, PLC/RF, and VLC/RF systems consider in this work with both worst device reshuffling and load balancing techniques. We also comment on the change in the association from initial to final (the association at which the SRC converges at a maximum value) in both the reshuffling techniques. Further, we present the numerical results to analyse the effect of increased number of SDs on the optimal SRC. Finally, we consider a practical scenario where there is a possibility for the PLC-disabled SDs that are not capable to connect to PLC APs. We consider a $10 \times 10 \times 3.5\,\text{m}^3$ indoor scenario [40]. In case of PLC, we choose $\xi = 0.1$, $\gamma = 10$, $G_p = 1$, $\delta = 40$ dB/KM, $N_p = 10^{-14}$ watts/Hz and $B_p = 10$ MHz [46]. For VLC, we choose $\psi = 60°$, $\delta = \beta = 0$, $A_d = 10^{-4}\,\text{m}^2$, $T_s(\beta) = g(\beta) = 1$, $N_v = 10^{-21}$ watts/Hz and $B_v = 100$ MHz. Finally, in the case of RF, the carrier frequency f_c is considered to be 2.4 GHz, $G_{h,r} = 1$, $N_r = 3.89 \times 10^{-21}$ watts/Hz and $B_r = 10$ MHz. Moreover, the transmit power, P_T, is considered as 10 mW for each AP belonging to any of the communication technology [1]. Further, the list of all parameters and corresponding values are tabulated in Table 1.

Figs. 4*a* and *b* show the SRC of all the considered hybrid communication systems with worst device reshuffling and load balancing techniques, respectively. From both, Figs. 4*a* and *b*, we observe that the proposed mechanism doubles the achievable SRC compared to the SNR-based AP association and BW allocation for most of the hybrid systems consider in this work. Further, the maximum SRC is achieved by the hybrid PLC/VLC/RF system among all communication systems under consideration. This observation is valid as, the aggregate BW of the hybrid PLC/VLC/RF system is higher than that of others. Moreover, we observe that the SRC of the hybrid VLC/RF system is higher than that of hybrid PLC/VLC and PLC/RF systems. This happens due to the combined effect of high SNR of the RF link and high BW of the VLC link for a fixed transmit power. Moreover, it is also evident that the initial SRC of hybrid PLC/VLC/RF and PLC/RF systems is higher compared to the other two hybrid systems under consideration. This is due to the fact that in these hybrid systems, the SDs are connected to both RF and PLC during the initial association as both RF and PLC provide relatively high SNR. However, in the case of hybrid VLC/RF and PLC/VLC systems, the SDs should associate to only RF and PLC, respectively, as both provide high SNR compared to the VLC system. This, in turn, reduces the achievable SRC in the initial association as all SDs associated to only RF and PLC in VLC/RF and PLC/VLC, respectively.

Fig. 5*a* shows the initial association of all SDs to the respective APs from which they receive higher SNR. Figs. 5*b* and *c* show the final association, at the saturated SRC, of the SDs with both worst device reshuffling and load balancing techniques, respectively. From Fig. 5*a*, it is observed that the number of SDs associated to PLC, VLC and RF are 3, 0, and 37, respectively. It is seen from the figure that all the SDs are connected to only PLC and RF during the initial association due to the provision of higher SNR by both PLC and RF compare to VLC. It has changed to 4, 7 and 29 with

Table 1 Summary of important parameters and their typical values used in this work

Notation	Definition	Value
$\mathscr{A}$	set of all APs	
A_d	area of the photodetector in VLC	$10^{-4}\,\mathrm{m}^2$
a	index of an AP	
$B_{a,n}$	BW allocated for the link between AP a and SD n	
$B_{a,\mathrm{max}}$	maximum available BW at AP a	
B_n	noise BW	100 MHz
B_p	allocated BW in PLC	10 MHz
B_r	allocated BW in RF	10 MHz
B_v	allocated BW in VLC	100 MHz
C	sum rate capacity (SRC)	
$\mathscr{D}$	set of PLC-disabled SDs	
d	distance between AP and SD	
f_c	carrier frequency in RF	2.4 GHz
$G_{h,\mathrm{r}}$	channel gain in RF	1
G_p	channel gain in PLC	1
$G_{\eta,\mathrm{r}}$	path gain in RF	
$g(\beta)$	gain of the concentrator in VLC	1
$H(0)$	DC channel gain in VLC	
I_2	noise BW factor	0.562
i	background current	$5100\,\mu\mathrm{A}$
k	number of VLC APs	4
l	number of PLC APs	3
N	number of SDs	40, 0–80
N_p	noise power spectral density in PLC	$10^{-14}\,\mathrm{watts/Hz}$
N_r	noise power spectral density in RF	$3.89 \times 10^{-21}\,\mathrm{watts/Hz}$
N_v	noise power spectral density in VLC	$10^{-21}\,\mathrm{watts/Hz}$
n	index of an SD	
P_n	noise power due to ISI	0
P_R	received power at an SD	
P_T	transmit power at an AP	10 mWatt
q	electronic charge	
R	resposivity of the photodiode in VLC	1
$T_\mathrm{s}(\beta)$	gain of optical filter in VLC	1
$\mathscr{U}$	set of all SDs	
$\mathscr{U}_a$	the number of SDs that are associated to AP a	
α	attenuation factor with distance in PLC	40 dB/KM
ξ	parameter of Bernoulli random variable n_b	0.1
γ	power ratio of impulsive noise to the background noise	10
Γ_p	signal-to-noise ratio (SNR) of PLC	
ρ	order of Lambert index in VLC	1
δ	the angle between the light emitting direction and light source normal direction in VLC	0°
β	incident angle of radiation in VLC	0°
β_c	field of view of the receiver in VLC	
ψ	LED's semi-angle at half power	60°
Γ_v	SNR in VLC	
η	path loss in RF	
$\Lambda_{a,n}$	binary indicator that defines the association of SD a to AP n	
$\Gamma_{a,n}$	SNR at SD n from AP a	
Ω	Lagrange multiplier	

worst device reshuffling technique and 7, 1 and 32 with load balancing technique as shown in Figs. 5b and c, respectively. This is due to the availability of excess BW and more APs has led to the increase in the number of SDs associated to the VLC APs at the saturated SRC.

Fig. 6 shows the numerical results that correspond to the variation of saturated SRC for the proposed hybrid system with respect to the increase of SDs. From figure, it is observed that the achievable saturated SRC increases linearly with the number of SDs and is maximum at $N = 60$. Further increase in the number of SDs decreases this value as can be observed from Fig. 6. It is also seen that the saturated SRC is slightly higher with load balancing technique compared to the worst device reshuffling technique. In the latter technique, the focus is on the reshuffling of the worst SD (worst individual sum rate) of all the SDs present in the system. In this case, the system can be left with a heavily loaded AP whose associated SDs can be further reshuffled to improve the achievable SRC. This is observed from Fig. 5b in which 7 SDs are associated
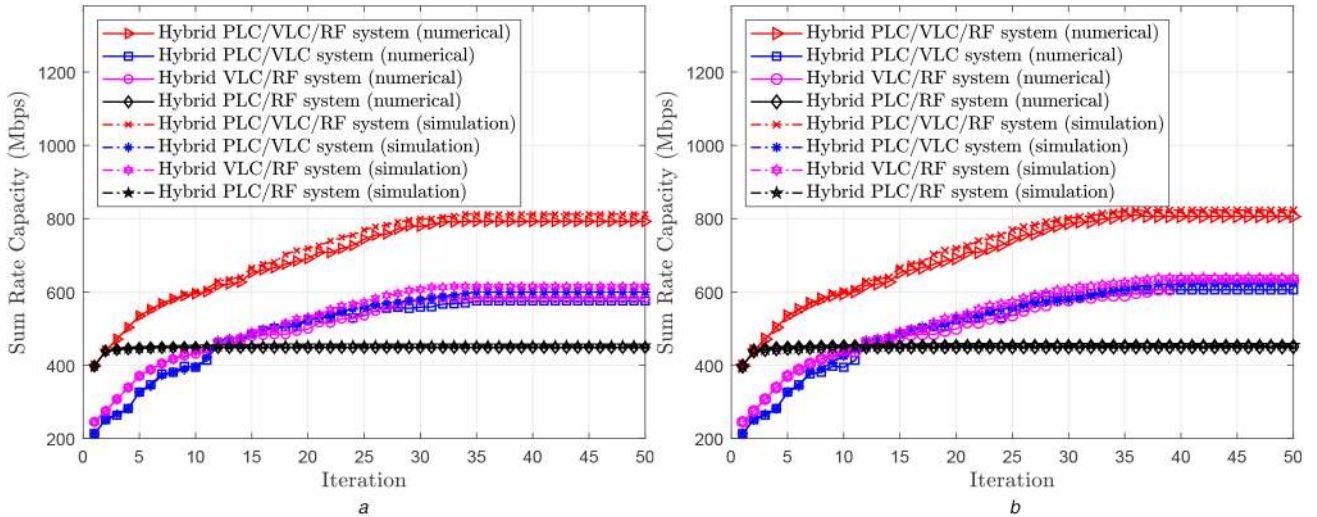
Fig. 4 *Sum rate versus iteration with*
(a) Worst device reshuffling, *(b)* Load balancing techniques with $N = 40$, $k = 4$, $l = 3$, and $\mathscr{D} = \{0\}$
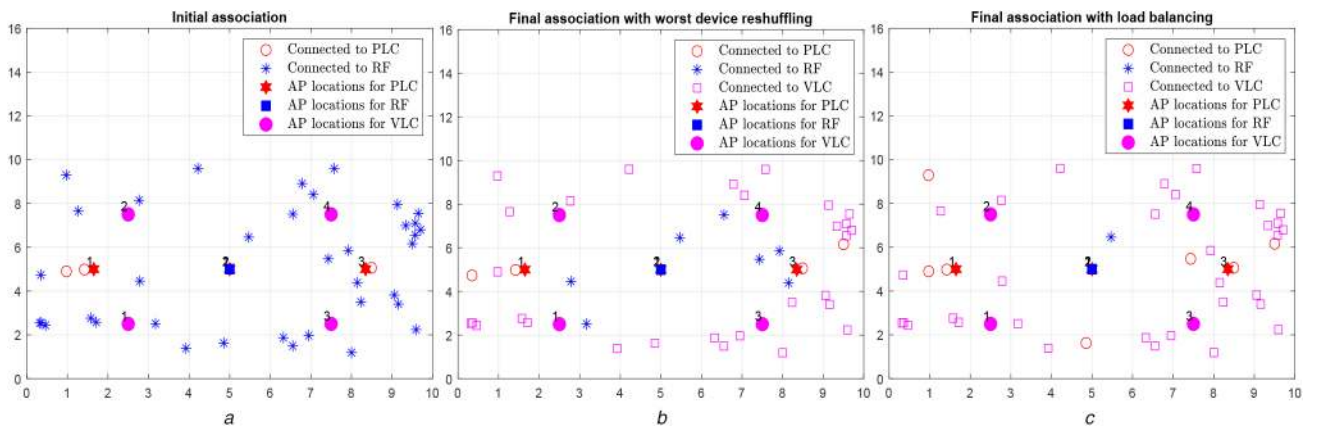

Fig. 5 *Association of each smart device with one of the communication technologies with*
(a) Initial association, *(b)* Final association with worst device reshuffling technique, *(c)* Final association with load balancing technique for the proposed hybrid PLC/VLC/RF system with $N = 40$, $k = 4$, $l = 3$, and $\mathscr{D} = \{0\}$
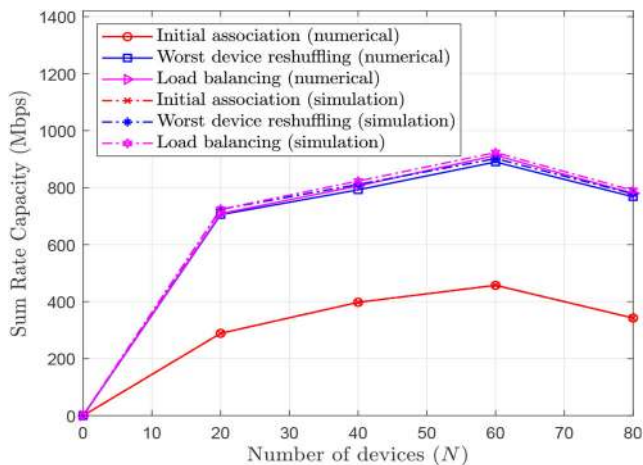

Fig. 6 *Maximum sum rate versus number of SDs with both worst device reshuffling and load balancing techniques with $k = 4$, $l = 3$, and $\mathscr{D} = 0$*

to RF at the saturation which can be further reshuffled to improve the achievable SRC. In the former technique, the focus is on balancing the load of each AP present in the system to achieve the saturated SRC as observed from Fig. 5c in which the number of SDs associated to RF has changed to 1.

Figs. 7a and b show numerical and simulation results that correspond to the SRC variation with worst device reshuffling and load balancing techniques, respectively, with an increased number of PLC-disabled SDs ($\mathscr{D}$) from a total number of 40 SDs. From

both Figs. 7a and b, we observe that the achievable SRC is maximum in the absence of PLC-disabled SDs ($\mathscr{D} = 0$) as all the SDs can connect to any communication system which improves the achievable SRC, whereas, the increase in the number of PLC-disabled SDs, $\mathscr{D}$, reduces the SRC due to the inefficient utilisation of the PLC system. Finally, the SRC is at its minimum value when all SDs are PLC-disabled as the hybrid system does not utilise PLC. Thus, it can be concluded that the addition of PLC in the system results in improved performance of the hybrid PLC/VLC/RF system in indoor scenarios.

5 Conclusion

In this paper, a hybrid PLC/VLC/RF fronthaul with a fibre-based wired backhaul system has been proposed to improve the achievable SRC. Wherein, an optimisation problem for the SRC has been formulated for the hybrid system in terms of AP association and BW allocation as the optimisation parameters and a hierarchical decomposition method has been considered to convert the non-linear optimisation problem into a set of convex optimisation problems. Then, efficient AP association and BW allocation strategies have been proposed to solve the optimisation problem in an iterative manner until the SRC converges to an optimal value. This iterative algorithm uses two reshuffling techniques such as the worst device reshuffling and the load balancing to obtain the saturated capacity. Further, an analytical approximation for the BW allocated to each SD for a given AP association has been derived using the Lagrangian multiplier method. Through extensive numerical results, it has been shown that the proposed algorithm doubles the achievable SRC compare
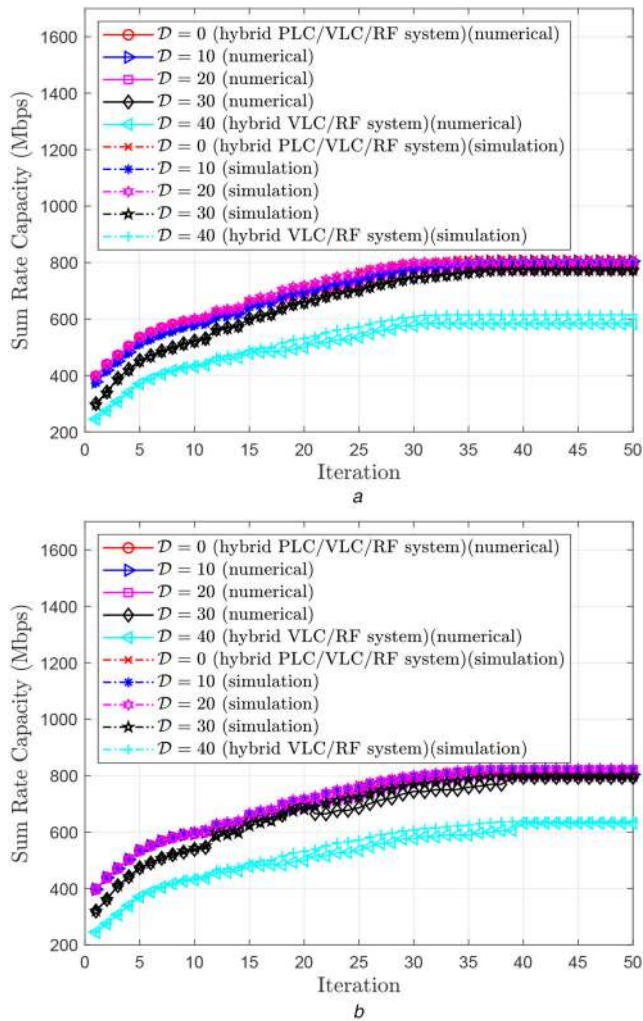
Fig. 7 *Sum rate versus iteration with respect to variable number of PLC-disabled SDs ($\mathcal{D}$) for*

(a) Worst device reshuffling, *(b)* Load balancing techniques with $N = 40$, $k = 4$, and $l = 3$

to the SNR-based AP association and BW allocation. It has also been concluded that the proposed hybrid PLC/VLC/RF system can considerably enhance the SRC in comparison to other hybrid combinations reported in the literature. Further, a practical scenario has also been considered, where, there exists PLC-disabled SDs that are only capable of connecting to either RF or VLC. Then, a numerical analysis has been presented on the achievable SRC to study the effect of an increased number of PLC-disabled SDs. Finally, the effect of the increase in the number of SDs on the optimal SRC is analysed numerically. It has been observed that the SRC is a concave function of the number of SDs. In future, we will analyse the system performance of the hybrid PLC/VLC/RF system with fibre optics as backhaul.

6 Acknowledgments

7 References

[1] Kashef, M., Abdallah, M., Al-Dhahir, N.: 'Transmit power optimization for a hybrid PLC/VLC/RF communication system', *IEEE Trans. Green Commun. Netw.*, 2018, **2**, (1), pp. 234–245

[2] Zeng, L., O'Brien, D., Le-Minh, H., *et al.*: 'Improvement of date rate by using equalization in an indoor visible light communication system'. Proc. IEEE Int. Conf. on Circuits and Systems for Communications, Shanghai, China, May 2008, pp. 678–682

[3] Komine, T., Nakagawa, M.: 'Integrated system of white LED visible–light communication and power–line communication', *IEEE Trans. Consum. Electron.*, 2003, **49**, (1), pp. 71–79

[4] Kashef, M., Torky, A., Abdallah, M., *et al.*: 'On the achievable rate of a hybrid PLC/VLC/RF communication system'. Proc. IEEE Global Communications Conf., San Diego, CA, December 2015, pp. 1–6

[5] Kuhn, M., Berger, S., Hammerstrom, I., *et al.*: 'Power line enhanced cooperative wireless communications', *IEEE J. Sel. Areas Commun.*, 2006, **24**, (7), pp. 1401–1410

[6] Sarafi, A.M., Tsiropoulos, G.I., Cottis, P.G.: 'Hybrid wireless–broadband over power lines: a promising broadband solution in rural areas', *IEEE Commun. Mag.*, 2009, **47**, (11), pp. 140–147

[7] Pan, Q.W., Kathnaur, A.: 'Power–line networks to extend ranges of 2.4 GHz wireless communications inside multi–storey buildings'. Proc. IEEE Radio and Wireless Symp., New Orleans, USA, January 2010, pp. 621–624

[8] Güzelgöz, S., Çelebi, H.B., Arsian, H.: 'Analysis of a multi–channel receiver: wireless and PLC reception'. Proc. European Signal Processing Conf., Aalborg, Denmark, August 2010, pp. 1106–1110

[9] Gheth, W., Rabie, K.M., Adebisi, B., *et al.*: 'Hybrid power–line/wireless communication systems for indoor applications'. Proc. Int. Symp. on Communication Systems, Networks & Digital Signal Processing, Budapest, Hungary, July 2018, pp. 1–6

[10] Komine, T., Haruyama, S., Nakagawa, M.: 'Performance evaluation of narrowband OFDM on integrated system of power line communication and visible light wireless communication'. Proc. Int. Symp. on Wireless Pervasive Computing, Phuket, Thailand, January 2006, pp. 6–11

[11] Song, J., Ding, W., Yang, F., *et al.*: 'Indoor hospital communication systems: an integrated solution based on power line and visible light communication'. Proc. IEEE Faible Tension Faible Consommation, Monaco, May 2014, pp. 1–6

[12] Alavi, S.E., Rezaie, H., Supa'at, A.S.M.: 'Application of OFDM on integrated system of visible free space optic with PLC'. Proc. IEEE Asia–Pacific Conf. on Applied Electromagnetics, Port Dickson, Malaysia, November 2010, pp. 1–5

[13] Ma, H., Lampe, L., Hranilovic, S.: 'Integration of indoor visible light and power line communication systems'. Proc. IEEE Int. Symp. on Power Line Communications and Its Applications, Johannesburg, South Africa, May 2013, pp. 291–296

[14] Gheth, W., Rabie, K.M., Adebisi, B., *et al.*: 'Performance analysis of integrated power–line/visible–light communication systems with AF relaying'. Proc. IEEE Global Communications Conf., Abu Dhabi, United Arab Emirates, December 2018, pp. 1–6

[15] Gheth, W., Rabie, K.M., Adebisi, B., *et al.*: 'On the performance of DF–based power–line/visible–light communication systems'. Proc. Int. Conf. on Signal Processing and Information Security, Dubai, United Arab Emirates, November 2018, pp. 1–4

[16] Basnayaka, D.A., Haas, H.: 'Hybrid RF and VLC systems: improving user data rate performance of VLC systems'. Proc. IEEE Vehicular Technology Conf. (VTC Spring), Glasgow, UK, May 2015, pp. 1–5

[17] Ma, X., Gao, J., Yang, F., *et al.*: 'Integrated power line and visible light communication system compatible with multi–service transmission', *IET Commun.*, 2017, **11**, (1), pp. 104–111

[18] Kashef, M., Ismail, M., Abdallah, M., *et al.*: 'Energy efficient resource allocation for mixed RF/VLC heterogeneous wireless networks', *IEEE J. Sel. Areas Commun.*, 2016, **34**, (4), pp. 883–893

[19] Ye, Q., Rong, B., Chen, Y., *et al.*: 'User association for load balancing in heterogeneous cellular networks', *IEEE Trans. Wirel. Commun.*, 2013, **12**, (6), pp. 2706–2716

[20] Lee, J.W., Mazumdar, R.R., Shroff, N.B.: 'Joint resource allocation and base–station assignment for the downlink in CDMA networks', *IEEE/ACM Trans. Netw.*, 2006, **14**, (1), pp. 1–14

[21] Zhang, H., Venturino, L., Prasad, N., *et al.*: 'Weighted sum–rate maximization in multi–cell networks via coordinated scheduling and discrete power control', *IEEE J. Sel. Areas Commun.*, 2011, **29**, (6), pp. 1214–1224

[22] Tan, C.W., Chiang, M., Srikant, R.: 'Fast algorithms and performance bounds for sum rate maximization in wireless networks', *IEEE/ACM Trans. Netw.*, 2013, **21**, (3), pp. 706–719

[23] Christensen, S.S., Agarwal, R., Carvalho, E.D., *et al.*: 'Weighted sum–rate maximization using weighted MMSE for MIMO–BC beamforming design', *IEEE Trans. Wirel. Commun.*, 2008, **7**, (12), pp. 4792–4799

[24] Chinnadurai, S., Selvaprabhu, P., Jiang, X., *et al.*: 'Worst–case weighted sum–rate maximization in multicell massive MIMO downlink system for 5G communications', *Phys. Commun.*, 2018, **27**, pp. 116–124

[25] Papaleonidopoulos, I.C., Capsalis, C.N., Karagiannopoulos, C.G., *et al.*: 'Statistical analysis and simulation of indoor single–phase low voltage power–line communication channels on the basis of multipath propagation', *IEEE Trans. Consum. Electron.*, 2003, **49**, (1), pp. 89–99

[26] Guzelgoz, S., Celebi, H.B., Arslan, H.: 'Statistical characterization of the paths in multipath PLC channels', *IEEE Trans. Power Deliv.*, 2011, **26**, (1), pp. 181–187

[27] Galli, S.: 'A novel approach to the statistical modeling of wireline channels', *IEEE Trans. Commun.*, 2011, **59**, (5), pp. 1332–1345

[28] Dubey, A., Mallik, R.K.: 'Effect of channel correlation on multi–hop data transmission over power lines with decode–and–forward relays', *IET Commun.*, 2016, **10**, (13), pp. 1623–1630

[29] Abou-Rjeily, C.: 'Performance analysis of power line communication systems with diversity combining under correlated lognormal fading and Nakagami noise', *IET Commun.*, 2017, **11**, (3), pp. 405–413

[30] Dubey, A., Mallik, R.K.: 'PLC system performance with AF relaying', *IEEE Trans. Commun.*, 2015, **63**, (6), pp. 2337–2345

[31] Sharma, D., Dubey, A., Mishra, S.*, et al.*: 'A frequency control strategy using power line communication in a smart microgrid', *IEEE Access*, 2019, **7**, pp. 21712–21721

[32] Reddy, Y.S., Dubey, A., Kumar, A.: 'A MAC–PHY cross–layer analysis of NB–PLC system in presence of impulsive noise'. Proc. Int. Conf. on Communication Systems & Networks, Bengaluru, India, January 2018, pp. 384–387

[33] Tan, Z., Liu, H.: 'Adaptive decision directed impulse noise mitigate in power line communication', *IET Signal Process.*, 2018, **12**, (3), pp. 368–374

[34] Rabie, K.M., Alsusa, E.: 'Preprocessing–based impulsive noise reduction for power–line communications', *IEEE Trans. Power Deliv.*, 2014, **29**, (4), pp. 1648–1658

[35] Komine, T., Nakagawa, M.: 'Fundamental analysis for visible–light communication system using LED lights', *IEEE Trans. Consum. Electron.*, 2004, **50**, (1), pp. 100–107

[36] Qiu, Y., Chen, H.-H., Meng, W.-X.: 'Channel modeling for visible light communications–a survey', *Wirel. Commun. Mob. Comput.*, 2016, **16**, (14), pp. 2016–2037

[37] Chen, S., Ma, X.: 'MIMO visible light communication system with block Markov superposition transmission', *IET Commun.*, 2018, **12**, (6), pp. 696–703

[38] Ding, J.P., Ji, Y.F.: 'Evolutionary algorithm–based optimisation of the signal–to–noise ratio for indoor visible–light communication utilising white light–emitting diode', *IET Optoelectron.*, 2012, **6**, (6), pp. 307–317

[39] Kafafy, M., Fahmy, Y., Khairy, M.: 'Optimising the inter–distance between transmitters in a multi–cell VLC system', *IET Commun.*, 2019, **13**, (7), pp. 811–817

[40] Stefan, I., Burchardt, H., Haas, H.: 'Area spectral efficiency performance comparison between VLC and RF femtocell networks'. Proc. IEEE Int. Conf. on Communications, Budapest, Hungary, June 2013, pp. 3825–3829

[41] Simon, M.K., Alouini, M.-S.: '*Digital communication over fading channels: a unified approach to performance analysis*' (John Wiley & Sons Inc., New York, 2004, 2nd edn.)

[42] Di Bert, L., Caldera, P., Schwingshackl, D.*, et al.*: 'On noise modeling for power line communications'. Proc. IEEE Int. Symp. on Power Line Communications and Its Applications, Udine, Italy, April 2011, pp. 283–288

[43] Wang, N., Hossain, E., Bhargava, V.K.: 'Joint downlink cell association and bandwidth allocation for wireless backhauling in two–tier HetNets with large–scale antenna arrays', *IEEE Trans. Wirel. Commun.*, 2016, **15**, (5), pp. 3251–3268

[44] Palomar, D.P., Chiang, M.: 'A tutorial on decomposition methods for network utility maximization', *IEEE J. Sel. Areas Commun.*, 2006, **24**, (8), pp. 1439–1451

[45] Antoniou, A., Lu, W.-S.: '*Practical optimization: algorithms and engineering applications*' (Springer Publishing Company, USA, 2007, 1st edn.)

[46] Dubey, A., Kundu, C., Ngatched, T.M.N.*, et al.*: 'Incremental relaying for power line communications: performance analysis and power allocation', *IEEE Syst. J.*, through early access, 2019, 1–12